Hindawi Publishing Corporation
Journal of Chemistry
Volume 2016, Article ID 6095023, 7 pages
http://dx.doi.org/10.1155/2016/6095023

Research Article

A Long-Chain Alkylation of Dialdehyde Starch to Improve Its Thermal Stability and Hydrophobicity

Jiang Zhu,[1,2] Zhaodong Wang,[2] Haitao Ni,[2] Xiang Liu,[2] Jian Ma,[2] and Jianxin Du[2]

[1]*Chongqing Key Laboratory of Environmental Materials and Remediation Technologies, ChongQing University of Arts and Sciences, Chongqing, China*
[2]*College of Materials and Chemical Engineering, Chongqing University of Arts and Sciences, Chongqing, China*

Correspondence should be addressed to Haitao Ni; htniok@163.com

Received 27 June 2016; Accepted 15 September 2016

Academic Editor: Alberto Ritieni

Hydrophobic dialdehyde starch (HDAS) was synthesized by dialdehyde starch (DAS) and eighteen-alkyl primary amine as the raw material in DMSO. The effect of the reaction conditions on the yield of HDAS was investigated such as catalyst content, reaction temperature, reaction time, and the in-feed molar ratio of -CHO/-NH_2. Moreover, the optimized test parameters were obtained by conducting orthogonal experiment. The molecular structure and the morphology of HDAS were characterized via Fourier transform infrared spectroscopy (FTIR) and scanning electron microscope (SEM). And the thermal stability and the hydrophobic properties of HDAS were investigated by thermal gravimetric analyzer (TG) and the hydrophobic testing. The results indicate that the yield of HDAS is the highest up to 44.21%, with feed composition 1 : 0.9, reaction temperature 40°C, reaction time 8 h, and acetic acid content 3%. And the introduction of the long-chain alkyl groups into the DAS backbones will ameliorate efficaciously the thermal stability and the hydrophobic properties of DAS, which almost has no effect on the DAS particle size.

1. Introduction

As a renewable resource, starch is considered to be fully biodegradable and nonpolluting to the environment. However, due to many hydroxyl groups on starch molecule, the strong intermolecular hydrogen bonding results in the fact that glass transition temperature is higher than the decomposition temperature, which is adverse for starch processability. Nevertheless, a large number of reactive hydroxyl groups in the molecular chains could provide a structural basis for the modification of starch. Various modification methods such as physically [1, 2], chemically [3, 4], or enzymatically [5–7] treating native starch with various reagents have been successfully used to overcome shortcomings and improve the inadequacy of starch. For example, among chemical modification methods, esterification and etherification have been reported to improve the thermal stability of starch [8, 9]. Oxidation is another chemical method for modifying starch and dialdehyde starch (DAS) is a very typical representative of the oxidized starches [10].

DAS has received much attention in recent decades because of its excellent physical, chemical, and biochemical properties. Since there is a great deal of reactive aldehyde group in the DAS molecular chains, DAS has been developed and widely used in many industries such as paper, textile, building materials, leather, medicine, and health. Nevertheless, the thermal stability of DAS is still a focusing point concerned in product processing [11]. Moreover, the decomposition temperature of DAS drops due to the poor thermal stability of the aldehyde group. It has been reported that dialdehyde yam starch has poor stability as compared to native starch when the content of the aldehyde groups is increased [12]. A recent study has also suggested that thermal stability of dialdehyde sweet potato starch will decrease when the aldehyde content was increased from 20% to 95% [13]. Therefore, knowing how to further improve the thermal stability of DAS is deserving of research. In the present study, our efforts involve attempting to improve the properties of DAS. Long-chain alkyl groups were introduced into the DAS backbones. Both the thermal stability and the hydrophobic

properties of DAS have significantly improved compared to its unmodified state.

2. Experimental

2.1. Material. DAS was purchased from Jinshan Modified Starch Co., Ltd (Shandong, China) and the content of aldehyde group (-CHO) in DAS was ascertained by the titration method as 23.1 wt%. Eighteen-alkyl primary amine was obtained from Jiayu Chemical Group (Shandong, China). Acetic acid (analytically pure) was supplied by Chongqing Chemical Reagent Factory (Chongqing, China). Dimethyl Sulfoxide (DMSO, analytically pure) and absolute ethyl alcohol (EA, analytically pure) were obtained from Kelong Chemical Co., Ltd (Chengdu, China).

2.2. Preparation of Hydrophobic Dialdehyde Starch (HDAS). HDAS was synthesized using eighteen-alkyl primary amine as the alkylating agent. A typical procedure was as follows: 3.00 g of DAS (bone dry) was added into a 100 mL flask with 25 mL DMSO and purged three times with dry nitrogen. Then, the flask was put into a preheated oil bath (T = 80°C) for about 30 min to obtain a homogenous melt system with strong stirring. And then, the mixture of eighteen-alkyl primary amine (5.79 g) and acetic acid (3 wt%) that was dissolved into 5 mL DMSO was syringed under nitrogen at 70°C and the reaction was allowed to proceed at the same temperature for 8 h defined as a reaction time. After quickly cooling to room temperature, the crude resultants were precipitated and washed three times by anhydrous ethyl alcohol. Then, the deposits were extracted with anhydrous ethyl alcohol in a Soxhlet apparatus for 48 h to remove impurities. Finally, the products were dried at 60°C in vacuum to constant weight. Yield was calculated as follows:

$$\text{Yield}\,(\%) = \frac{m}{m_1 + m_2} \times 100\%, \tag{1}$$

where m_1 is the mass of dry DAS; m_2 is the mass of eighteen-alkyl primary amine; m is the mass of the target products.

2.3. Characterization. Fourier transform infrared spectra (FTIR) of all samples after drying in a vacuum oven at 60°C for 48 h were carried out by a FTIR spectrometer (Thermo Fisher Corp., Nicollet 6670, USA), using infrared attenuated total reflection (IRATR) and operating in the wavenumber range 4,000–500 cm^{-1} with 4 cm^{-1} resolution and 32 scanning times.

The morphology of the selective specimen was evaluated by a scanning electron microscope (SEM) (Philips XL-3, FEI, Oregon, USA). The SEM images were obtained after the sputter coating of gold particles about a thickness of 10 nm at an accelerating voltage of 20 kV with a lanthanum hexaboride (LaB_6) crystal as electron emitter.

The thermal stability of the products was performed by a NETZSCH device TG 209 F1 at a heating rate of 10°C min^{-1} under nitrogen atmosphere from 40°C to 600°C.

2.4. Hydrophobic Testing of DAS and HDAS. A typical procedure to investigate hydrophobicity of samples was as follows [14]: firstly, the selective sample (bone dry) with a certain weight defined as W_0 was put into a vial. Then, the deionized water was added into the system and was sonicated at 50°C for 30 min to obtain the certain concentration of the resulting mixture (30 mg/mL). After a systematic testing time, the suspension was precipitated and the deposits were dried at 60°C in vacuum to constant weight. Finally, the sample was weighted with the analytical balance, defined as W_D. Weight loss (W_l) was calculated as follows:

$$W_l\% = \frac{W_0 - W_D}{W_0} \times 100. \tag{2}$$

3. Results and Discussion

3.1. Analysis of the Reactivity for Preparing HDAS. For the sake of investigating the effect of reaction conditions on the yield of HDAS such as acetic acid content, reaction temperature, reaction time, and the in-feed molar ratio of -CHO/-NH_2, a trial of the products was synthesized. And then, the optimal conditions were obtained through orthogonal experiment. The detailed reaction conditions were exhibited in Figure 1 and the results of orthogonal experiment were summarized in Table 1.

Figure 1(a) showed the variations of yields of the products as a function of the different amount of acetic acid, which was carried out in which the molar ratio of -CHO/-NH_2 was fixed at 1 : 0.5, the reaction temperature was 50°C, and the reaction time was 4 h. From the plots, we found that yields of HDAS almost progressively increased with the increment of catalyst in the range from 1 wt% to 3 wt% (based on DAS). It indicated that the nucleophilic addition of -CHO of the DAS backbone took place more easily within this content range, owing to the rapid augment of the propagating centers. When it was beyond 3 wt%, yields of the products were almost invariant. This indicated that the excessive amount of acetic acid was not beneficial for introduction of the long-chain alkyl amine onto the DAS backbone.

Figure 1(b) depicted the changing behaviors of yields of HDAS with a lapse of reaction time at the fixed molar ratio of -CHO/-NH_2, catalyst, and reaction temperature (-CHO/-NH_2: 1 : 0.5, acetic acid: 3 wt%, and reaction temperature: 50°C). We can see clearly that at the earlier stage of the reaction, the yields of the target products increased monotonically within 4–8 h. This phenomenon meant that the active aldehyde groups of the DAS backbone can play a role as the propagating centers to initiate the reaction easily. However, the yields of the products decreased rapidly when 120 min elapsed, and then it gradually decreased while the reaction time was further increased. The results indicated that, in the latter period of the reaction, the prolongation of reaction time made the decomposition reaction of the products easier.

Figure 1(c) exhibited the effect of different reaction temperatures on the yields of HDAS (-CHO/-NH_2: 1 : 0.5, acetic acid: 3 wt%, and reaction time: 4 h). It was found that the yields slightly increased in the earlier stage from 30°C to 40°C. The yield of HDAS reached the maximum at 40°C and then decreased greatly above this temperature. It could be explained that the higher reaction temperature

Table 1: Results of orthogonal test.

Number	Figure 1(d) in-feed molar ratio (mol/mol)	Figure 1(c) reaction temperature (°C)	Figure 1(b) reaction time (h)	Figure 1(a) acetic acid content (%)	Yield (%)
1	1 : 0.5	40	4	1	40.21
2	1 : 0.7	50	8	1	32.09
3	1 : 0.9	60	10	1	28.78
4	1 : 0.9	40	8	3	44.21
5	1 : 0.5	50	10	3	30.03
6	1 : 0.7	60	4	3	34.22
7	1 : 0.7	40	10	4	35.15
8	1 : 0.9	50	4	4	25.71
9	1 : 0.5	60	8	4	38.26
$K1$	36.17	39.86	33.38	33.69	
$K2$	33.82	29.28	38.19	36.15	
$K3$	32.90	33.75	31.01	33.04	
R	3.27	10.58	7.18	3.11	

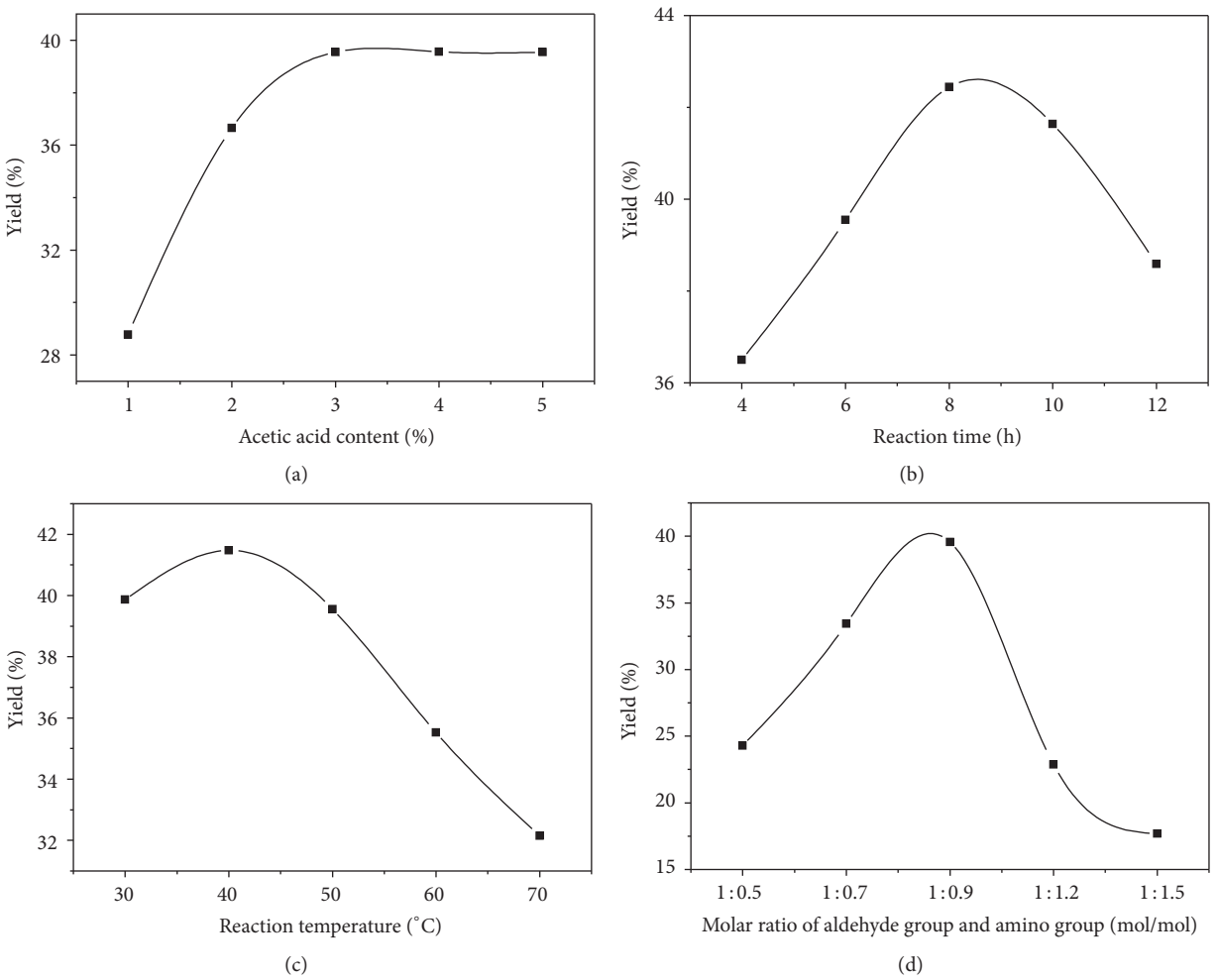

Figure 1: The effect of reaction conditions on the yield of HDAS.

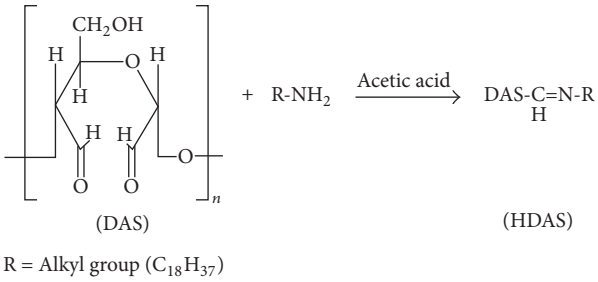

Scheme 1: Preparation process of HDAS.

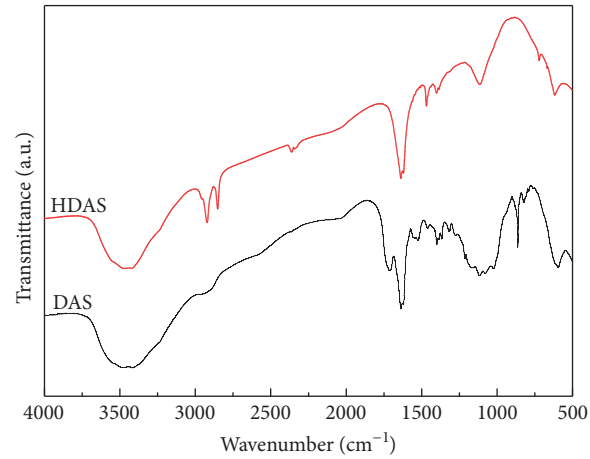

Figure 2: FTIR analysis of DAS and HDAS.

was helpful to enhance the reaction rate until the reaction converged to equilibrium with the gradual consumption of aldehyde groups of the DAS backbone. However, when the reaction temperature was too high to break the equilibrium, the thermal depolymerization of the products took place more easily.

Figure 1(d) shows the changing behaviors of yields of HDAS with the variation of the in-feed molar ratio of -CHO/-NH_2 (acetic acid: 3 wt%, reaction time: 4 h, and reaction temperature: 40°C). From the plots, we found that yields of HDAS almost increased in proportion to the amount of PDO monomer in-feed in the range from 1 : 0.5 to 1 : 0.9. And the highest value of 38.8% was reached at the molar ratio of 1 : 0.9; however, the yield declined when the molar ratio of -CHO/-NH_2 was 1 : 0.9. It could be said that the increase of reactant concentration was propitious to improve the reaction rate. However, with the gradual consumption of aldehyde groups of the DAS backbone, the excessive amount of the long-chain alkyl amine would not complete the nucleophilic addition with the residual aldehyde groups of the DAS backbone.

Based on the above experiments, the method of orthogonal test was further used to optimize the preparation process of HDAS. It is well known that orthogonal test is a high-efficiency method for designing the experiment, which is used to investigate the multifactor, multilevel experiment. And the optimum conditions can be obtained through selecting the representative sample from a comprehensive test based on the orthogonality. The results of orthogonal test were depicted in Table 1, where $K1$, $K2$, and $K3$ represented the mean values of the HDAS yields in different factors and different levels. R expressed the difference value between maximum and minimum values of $K1$, $K2$, and $K3$. From the data, we can find that the optimum reaction conditions for preparing HDAS were the in-feed molar ratio of -CHO/-NH_2 of 1 : 0.9, reaction temperature of 40°C, reaction time of 8 h, and the acetic acid content of 3 wt%, respectively. So, in this paper, the impact level of these four factors was as follows: reaction temperature > reaction time > the in-feed molar ratio of -CHO/-NH_2 > the acetic acid content.

3.2. Chemical Structures of HDAS. The preparation of HDAS was performed using a nucleophilic addition reaction between the aldehyde groups and the amino groups [15]. The synthesis process was exhibited in Scheme 1. When the aldehyde groups react with primary amine in the existence of acetic acid, the oxygen of the aldehyde groups is first protonated to become the oxonium ions by the acetic acid, and then these react with the nitrogen atoms of the amino groups in primary amine by the nucleophilic addition. Finally, the reactants complete the dehydration to obtain the target products.

Figure 2 depicted the FTIR spectra of DAS and HDAS. It can be seen that there were characteristic peaks belonging to the DAS backbones [4, 16]. The broad peak around 3400 cm^{-1} was assigned to the -OH stretching vibration. And the peak at 1712 cm^{-1} was ascribed to the characteristic stretching vibration of C=O in DAS backbones. In addition, the strong peak at 1630 cm^{-1} can be attributed to the -OH bending vibration due to the existence of the water molecular [17]. After the introduction of the long-chain alkyl groups, we can see that the absorption band at 1712 cm^{-1} vanished in the curve of HDAS. And one may not be able to differentiate between the absorption bands at 1630 cm^{-1} due to -OH and C=N, because their absorptions peaks may overlap. Besides, the strong peaks around 2920 cm^{-1} and 2840 cm^{-1} were assigned to the characteristic -CH_2- and -CH_3 stretching vibration, respectively. The peak at 1460 cm^{-1} was ascribed to the -CH_2- bending vibration. And the peak at 1100 cm^{-1} was attached to the C-O stretching vibration, originating from the starch backbone. These results mean that the nucleophilic addition reaction was performed successfully.

3.3. Morphology of HDAS. The morphology of HDAS was investigated by scanning electron microscopy and is exhibited in Figure 3. The DAS sample was chosen for analysis of the morphological variations of HDAS after modifying. From the SEM photos, we can see clearly that most DAS particles were irregular sphere and about 10 μm in diameter (seen in Figure 3(a)). And the surface of DAS particles (Figure 3(b)) was relatively smooth; at the same time the phase interface was distinct between these particles. As far as the HDAS particle was concerned (Figures 3(c) and 3(d)), HDAS particles retained their spherical shapes, whose particle size was nearly the same as those of DAS, originating from the DAS substrate. However, from Figure 3(d), one can distinctly see that the

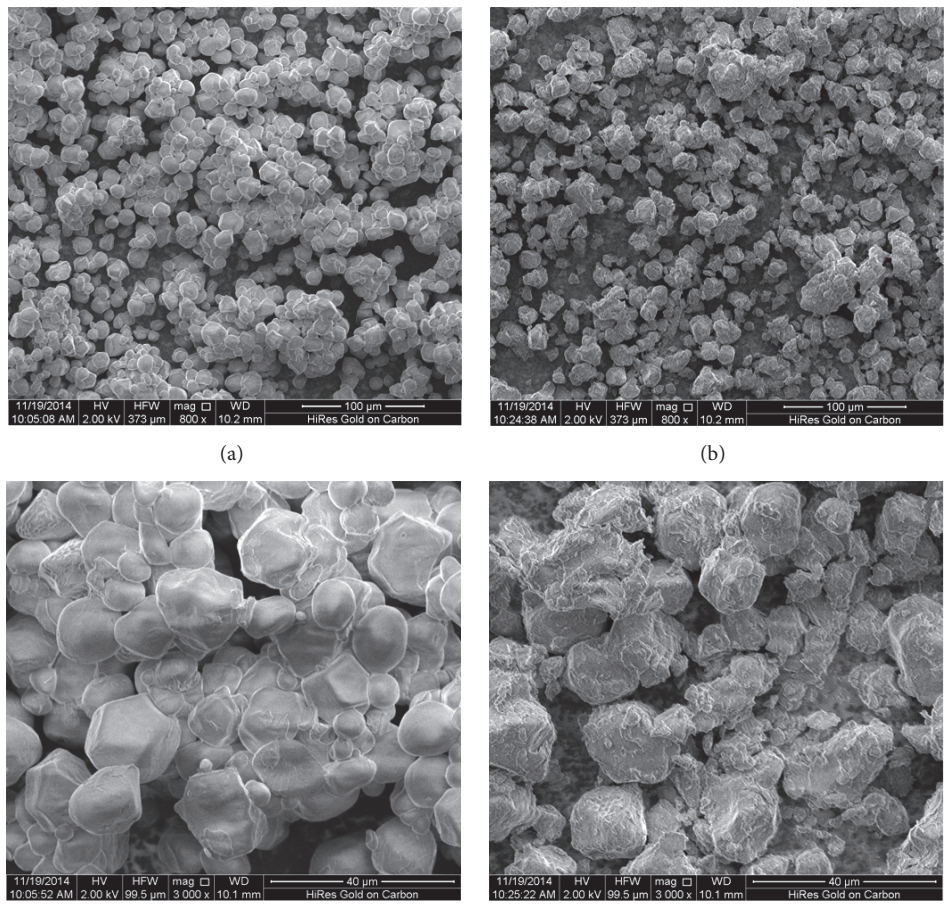

Figure 3: The morphology of DAS (a, c) and HDAS (b, d).

surface of HDAS was irregular and rough, coated by a large amount of flaky materials. In this paper, it can be said that the long-chain alkyl groups were introduced successively into the DAS backbones.

3.4. Thermal Stability of HDAS. The thermal stability of DAS and HDAS was examined by thermogravimetry (TG) in N_2 atmosphere at a heating rate of 10°C/min, and the TGA and DTG curves of the selective samples were shown in Figure 4. Obviously, it can be observed that both DAS and HDAS almost exhibited three decomposition ranges. One decomposition range was found where the maximal decomposition temperature was around 100°C, which belonged to the weight loss of water in samples in their TG curves (seen in Figure 4(a)) [18, 19]. It was distinct that compared with that of DAS, this decomposition range of HDAS was ameliorated for the introduction of the hydrophobic long-chain alkyl groups in the DAS backbone. And the next decomposition range can be seen at around 200°C in the DAS TG curve. It was interesting that DAS rapidly reached its maximum weight-loss rate (−11.4%/min) and completed the last decomposition range at around 300°C after finishing the second decomposition range (seen in Figure 4(b)). It could be said that the strong hydrogen-bond interaction in starch backbones was destroyed by the oxidation in the preparing process of DAS. So, the DAS backbones became weak to easily decompose with the increase of decomposition temperature. However, in contrast with that of DAS, the TG curve of HDAS got placid and attained its maximum weight-loss rate of 7.1%/min with the increment of decomposition temperature at around 300°C. It meant that due to the introduction of the long-chain alkyl groups onto DAS backbones, the thermal stability of DAS was further improved, which caused some DAS to degrade after 400°C.

3.5. Hydrophobic Properties of HDAS. Contact angle measurements have been used to investigate the relative hydrophilicity or hydrophobicity of materials [20]. Before the contact angle measurements, both DAS and HDAS powder samples were pressed to be a round disc. The measurements of contact angle of water on the selective discs were performed by a sessile drop method (exhibited in Figure 5) [21]. Although the water contact angle of DAS was almost investigated, the corresponding angle of HDAS was ~70°. In this paper, it means that the introduction of the long-chain alkyl groups could give a hydrophobic character of DAS.

Figure 6 demonstrated the hydrophobic testing of DAS and HDAS. From the plots, one can find that the weight loss

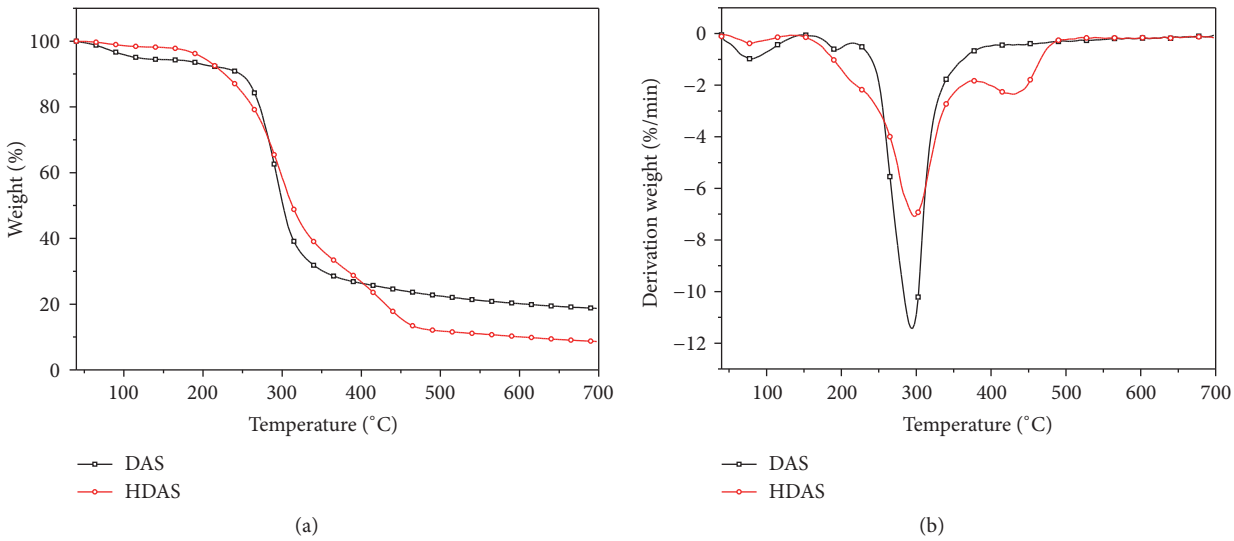

Figure 4: TGA and DTG curves of DAS and HDAS.

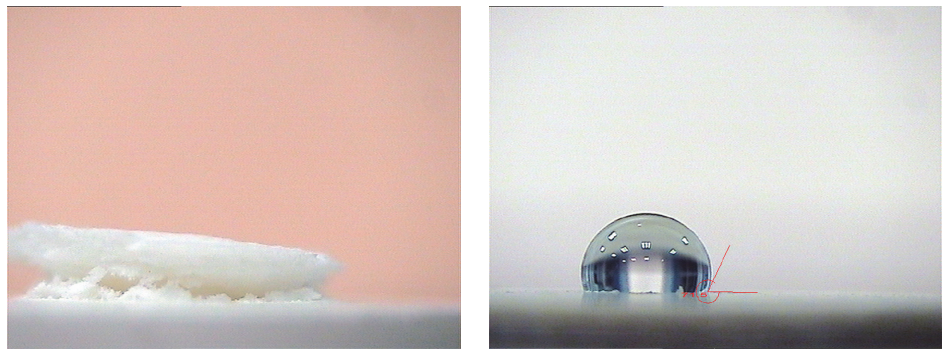

Figure 5: The measurements of contact angle of water on DAS (a) and HDAS (b).

of DAS and HDAS increased monotonously with the increase of testing time. And when the testing time was 3 days, the weight loss of the selective samples all reached the maximum of 68.9% and 37.5% for DAS and HDAS, respectively. The weight-loss values were almost invariant after 3 days for DAS and HDAS. This indicates that the introduction of the long-chain alkyl groups onto DAS backbone can obviously improve the hydrophobicity of DAS. In this work, it can be plausible that for the existence of abundant hydroxyl groups in DAS backbones, there is strong hydrogen-bond interaction between hydroxyl groups and water molecules, leading to improving the solubility of DAS in water. Nevertheless, when the long-chain alkyl groups are introduced onto DAS backbones, these hydrophobic groups impair the hydrogen bonding between hydroxyl groups and water molecules. Thus, the weight loss of HDAS is lower than that of DAS in the hydrophobic testing.

4. Conclusions

HDAS could be successfully prepared by the nucleophilic addition reaction between DAS and eighteen-alkyl primary amine. Within an appropriate range of conditions, such as catalyst content, reaction temperature, reaction time, and the in-feed molar ratio of -CHO/-NH_2, these conditions could all promote the yield of HDAS. The optimum conditions were as follows: the in-feed molar ratio of -CHO/-NH_2 of 1 : 0.9, reaction temperature of 40°C, reaction time of 8 h, and acetic acid content of 3 wt%, respectively. The yield of HDAS prepared under the above conditions had maximum of 44.2%.

HDAS prepared under the above conditions almost retained the same particle size just like that of DAS substrate, but its surface became rough. And the introduction of the long-chain alkyl groups into the backbones of DAS could improve the thermal stability of DAS, which caused some DAS to degrade after 400°C. The results of the hydrophobic testing indicated that the long-chain alkyl groups can obviously ameliorate the hydrophobicity of HDAS after the nucleophilic addition reaction, twice as much as the original DAS.

Competing Interests

The authors declare that they have no competing interests.

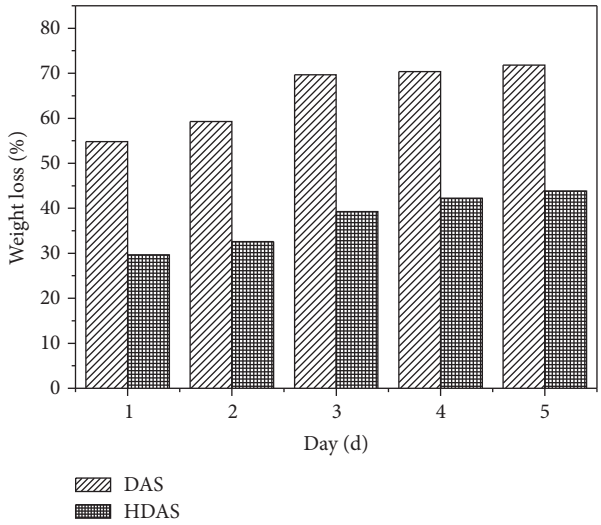

Figure 6: Hydrophobicity testing of DAS and HDAS.

Acknowledgments

This study was financially supported by (a) the Science and Technology Project Affiliated to Chongqing Municipal Education Department (Grant no. KJ1401122) and (b) the Local Fund for Chongqing University of Arts and Sciences (Grants nos. R2012CH09 and R2012CH12).

References

[1] A. R. Jambrak, Z. Herceg, D. Šubarić et al., "Ultrasound effect on physical properties of corn starch," *Carbohydrate Polymers*, vol. 79, no. 1, pp. 91–100, 2010.

[2] J. Y. Zuo, K. Knoerzer, R. Mawson, S. Kentish, and M. Ashokkumar, "The pasting properties of sonicated waxy rice starch suspensions," *Ultrasonics Sonochemistry*, vol. 16, no. 4, pp. 462–468, 2009.

[3] J. Yu, P. R. Chang, and X. Ma, "The preparation and properties of dialdehyde starch and thermoplastic dialdehyde starch," *Carbohydrate Polymers*, vol. 79, no. 2, pp. 296–300, 2010.

[4] M. Fiedorowicz and A. Para, "Structural and molecular properties of dialdehyde starch," *Carbohydrate Polymers*, vol. 63, no. 3, pp. 360–366, 2006.

[5] R. F. Tester, J. Karkalas, and X. Qi, "Starch structure and digestibility enzyme-substrate relationship," *World's Poultry Science Journal*, vol. 60, no. 2, pp. 186–195, 2004.

[6] M. M. Kasprzak, H. N. L. Lærke, F. H. Larsen, K. E. B. Knudsen, S. Pedersen, and A. S. J. Jørgensen, "Effect of enzymatic treatment of different starch sources on the *in vitro* rate and extent of starch digestion," *International Journal of Molecular Sciences*, vol. 13, no. 1, pp. 929–942, 2012.

[7] J. Blazek and E. P. Gilbert, "Effect of enzymatic hydrolysis on native starch granule structure," *Biomacromolecules*, vol. 11, no. 12, pp. 3275–3289, 2010.

[8] H. Staroszczyk, P. Tomasik, P. Janas, and A. Poreda, "Esterification of starch with sodium selenite and selenate," *Carbohydrate Polymers*, vol. 69, no. 2, pp. 299–304, 2007.

[9] M. A. Misman, A. R. Azura, and Z. A. A. Hamid, "Physicochemical properties of solvent based etherification of sago starch," *Industrial Crops and Products*, vol. 65, pp. 397–405, 2015.

[10] X. He and D. F. Wang, "Effects of internal factors on surface wettability of corn stalk rind," *International Journal of Agricultural and Biological Engineering*, vol. 8, no. 6, pp. 77–83, 2015.

[11] S.-D. Zhang, X.-L. Wang, Y.-R. Zhang, K.-K. Yang, and Y.-Z. Wang, "Preparation of a new dialdehyde starch derivative and investigation of its thermoplastic properties," *Journal of Polymer Research*, vol. 17, no. 3, pp. 439–446, 2010.

[12] L. Zhang, P. Liu, Y. Wang, and W. Gao, "Study on physicochemical properties of dialdehyde yam starch with different aldehyde group contents," *Thermochimica Acta*, vol. 512, no. 1-2, pp. 196–201, 2011.

[13] S. Zhang, F. Liu, H. Peang, and Y. Wang, "An investigation of the effect of semi-acetal formation on the properties of dialdehyde starch and its thermoplastic blend with glycerol," *Journal of Macromolecular Science, Part B*, vol. 54, no. 7, pp. 836–850, 2015.

[14] J. Jin, M. Song, and D. J. Hourston, "Novel chitosan-based films cross-linked by genipin with improved physical properties," *Biomacromolecules*, vol. 5, no. 1, pp. 162–168, 2004.

[15] C. Godoy-Alcántar, A. K. Yatsimirsky, and J.-M. Lehn, "Structure-stability correlations for imine formation in aqueous solution," *Journal of Physical Organic Chemistry*, vol. 18, no. 10, pp. 979–985, 2005.

[16] S.-D. Zhang, Y.-R. Zhang, J. Zhu, X.-L. Wang, K.-K. Yang, and Y.-Z. Wang, "Modified corn starches with improved comprehensive properties for preparing thermoplastics," *Starch*, vol. 59, no. 6, pp. 258–268, 2007.

[17] I. V. Vorotyntsev, I. I. Grinvald, I. Y. Kagalaev et al., "IR spectroscopic study of the complex formation between ammonia and water molecules in a KBr matrix," *Russian Journal of Physical Chemistry A*, vol. 88, no. 4, pp. 625–628, 2014.

[18] M.-F. Huang, J.-G. Yu, and X.-F. Ma, "Studies on the properties of Montmorillonite-reinforced thermoplastic starch composites," *Polymer*, vol. 45, no. 20, pp. 7017–7023, 2004.

[19] P. Mokrejs, F. Langmaier, D. Janacova, M. Mladek, K. Kolomaznik, and V. Vasek, "Thermal study and solubility tests of films based on amaranth flour starch-protein hydrolysate," *Journal of Thermal Analysis and Calorimetry*, vol. 98, no. 1, pp. 299–307, 2009.

[20] J. H. Bae and S. H. Kim, "Alkylation of mixed micro- and nanocellulose to improve dispersion in polylactide," *Polymer International*, vol. 64, no. 6, pp. 821–827, 2015.

[21] G. L. Mack and D. A. Lee, "The determination of contact angles from measurements of the dimensions of small bubbles and drops. II. The sessile drop method for obtuse angles," *The Journal of Physical Chemistry*, vol. 40, no. 2, pp. 169–176, 1936.